Publications of the Korean Astronomical Society
**27**: 291 ∼ 292, 2012 September

ISSN 1225-1534 (Print)
http://dx.doi.org/10.5303/PKAS.2012.27.4.291

# SED DECOMPOSITION OF INFRARED-LUMINOUS GALAXIES

Jong Chul Lee[1,2]
[1]Department of Physics and Astronomy, Seoul National University, Seoul 151-747, Korea
[2]Korea Astronomy and Space Science Institute, Daejeon 305-348, Korea
*(Received July 02, 2012; Accepted August 17, 2012)*

## ABSTRACT

We select infrared-luminous galaxies by cross-matching the SDSS spectroscopic sample of galaxies with the *WISE* all-sky survey catalog. Based on photometric data points covering from SDSS $u$-band to *WISE* 22 $\mu$m, their spectral energy distributions (SEDs) are separated into AGN, elliptical, spiral, and irregular galaxy components. The derived luminosities of spiral galaxy and AGN are well correlated with H$\alpha$ and [OIII] line luminosities, respectively. Most galaxies are dominated by young stellar populations even for optical AGNs, but at least 10% of optical non-AGNs appear to harbor buried AGNs. The AGN contribution increases dramatically with the total luminosity. These results show that the SED decomposition is successful and is useful to understand the true nature of dusty galaxies.

*Key words:* galaxies: active; galaxies: starburst; infrared: galaxies

## 1. INTRODUCTION

In the early Universe, galaxies grow via gas-rich major mergers triggering starburst and nuclear activity. Ultraluminous infrared galaxies (ULIRGs; $L_{\rm IR\ (8-1000\ \mu m)} \geq 10^{12}\ L_{\odot}$) are suspected to be at such a stage in the sense that a significant fraction of ultraviolet light associated with the activity is converted to infrared light by thermal processes of dust grains. In order to investigate the primary energy source (i.e., star formation, SF, vs. active galactic nucleus, AGN) in dusty galaxies, various diagnostic diagrams have been used (e.g., Veilleux et al., 2009; Lee et al., 2011). It is now possible to quantify the relative contribution of SF and AGN based on spectral energy distribution (SED) decomposition (e.g., Mullaney et al., 2011; Donoso et al., 2012). In this work, we construct a large sample of infrared-luminous galaxies using SDSS data and recently released *WISE* (*Wide-field Infrared Survey Explorer*) all-sky survey data. After separating their SEDs into young and old stellar populations plus AGN, we provide information on the typical contributions of each component.

## 2. DATA AND ANALYSIS

Our sample was based on the SDSS DR7 galaxies whose optical spectra are available. Their infrared counterparts were found in the *WISE* source catalog within 3 arcsec. We selected galaxies which are detected in the SDSS $ugriz$-bands and *WISE* 3.4, 4.6, 12, 24 $\mu$m above 5$\sigma$ levels. Among them, we focused on galaxies with a narrow range of redshift ($0.04 < z < 0.2$) to reduce the aperture-related effects and with signal-to-noise ratio > 5 of emission line fluxes H$\beta$, [OIII]$\lambda$5007, H$\alpha$, and [NII]$\lambda$6584 for reliable spectral classification in the BPT diagram (Baldwin, Phillips, & Terlevich, 1981). The resultant sample contains 59,046 infrared-luminous galaxies.

In order to analyze their SEDs we used the four empirical SED templates spanning the wavelength range from 0.03 to 30 $\mu$m and the fitting code of Assef et al. (2010): $L_{\rm bol\ (0.03-30\ \mu m)} = L_{\rm AGN} + L_{\rm E} + L_{\rm Sbc} + L_{\rm Im}$. Each template represents AGN (non-stellar contribution), elliptical (old stellar population), spiral (continuously star-forming), and irregular (starbursting) galaxies. The fitting code was applied to the 9 photometric data points by allowing variation of dust-extinction.

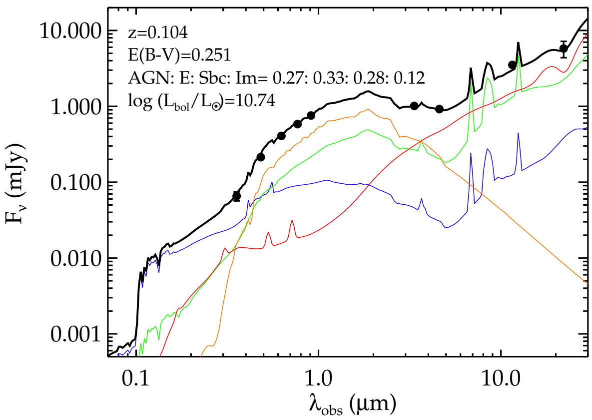


**Fig. 1.** An example of the SED fits. The labels indicate the contributions (to the bolometric luminosity) of the templates, which are shown in red (AGN), orange (E), green (Sbc), and blue (Im) lines. The black line and circles (with error bars) represent the total SED and observed photometric data points.

Figure 1 shows an example of the SED fits. Based on Monte-Carlo simulations with photometric errors we estimate that the uncertainty associated with the contribution of each component to $L_{\rm bol}$ is typically $\sim$2%, while the contribution uncertainties to $L_{12}$ and $L_{22}$ (monochromatic luminosities, $\nu L_\nu$, at rest-frame wavelength 12 and 22 $\mu$m) are $\sim$6%.

## 3. RESULTS

We found that H$\alpha$ and [OIII] luminosities, after aperture and extinction corrections, are best correlated with the derived luminosities of Sbc and AGN components, respectively (Spearman rank correlation coefficient = 0.83 and 0.63). By considering that H$\alpha$ and [OIII] emission lines are known to trace star formation and nuclear activity, the finding implies that the SED decomposition is successful. This is also supported by the fact that the mean AGN contribution is higher in optically more AGN-like galaxies (3.0% for star-forming; 6.0% for composite; 15.9% for AGN). Interestingly 15.8% of star-forming galaxies show non-negligible ($>$ 5%) AGN contributions, which could be regarded as optically buried AGNs.

The mean contributions of each component to $L_{\rm bol}$ ($L_{22}$) in bins of optical spectral type and $L_{\rm bol}$ ($L_{22}$) are listed in Table 1. Although most of the infrared-luminous galaxies are dominated by young stellar components even for optical AGNs, the mean AGN contribution increases dramatically with the luminosity, so that AGNs become a significant power source in the most luminous ones, corresponding to ULIRGs. We note that the trends in $L_{12}$ are similar to those in $L_{22}$ but the old stellar population contribution is up to a few percent.

Table 1.

Mean Contributions of Each Component to $L_{\rm bol}$ ($L_{22}$) in Bins of Optical Spectral Type and $L_{\rm bol}$ ($L_{22}$)

| $L_{\rm bol}$ | Star-forming | Composite | AGN |
|---|---|---|---|
| 10.0–10.3 | 02.1 18.0 34.0 45.9 | 04.2 38.3 38.6 18.8 | 07.5 45.7 29.1 17.7 |
| 10.3–10.6 | 02.0 17.8 37.7 42.5 | 03.7 35.7 38.0 22.6 | 09.7 44.4 26.2 19.8 |
| 10.6–10.9 | 02.7 15.7 43.1 38.5 | 04.4 34.0 37.1 24.6 | 10.6 43.7 24.1 22.6 |
| 10.9–11.2 | 04.5 12.1 50.3 33.1 | 06.7 28.8 39.5 24.9 | 14.1 39.7 23.5 22.6 |
| 11.2–11.5 | 11.6 08.5 52.9 27.0 | 16.9 20.1 41.1 22.0 | 31.5 32.1 18.9 17.5 |
| $L_{22}$ | Star-forming | Composite | AGN |
| 09.0–09.4 | 02.4 00.2 53.4 44.1 | 05.8 00.6 52.9 40.7 | 10.1 00.9 37.1 51.8 |
| 09.4–09.8 | 02.9 00.1 67.0 30.0 | 07.1 00.3 66.0 26.5 | 20.1 00.5 50.0 29.5 |
| 09.8–10.2 | 05.4 00.1 73.4 21.1 | 09.8 00.2 72.8 17.3 | 28.9 00.3 53.2 17.6 |
| 10.2–10.6 | 13.5 00.0 71.0 15.5 | 15.8 00.1 72.7 11.4 | 39.1 00.2 49.4 11.3 |
| 10.6–11.0 | 45.8 00.0 43.9 10.3 | 38.1 00.0 55.4 06.5 | 65.3 00.1 28.8 05.8 |

The values represent the mean contributions (%) of AGN, elliptical, spiral, and irregular galaxy components in each bin.

## REFERENCES

Assef, R. J., et al., 2010, Low-Resolution Spectral Templates for Active Galactic Nuclei and Galaxies from 0.03 to 30 $\mu$m, ApJ, 713, 970

Baldwin, J. A., Phillips, M. M., & Terlevich, R., 1981, Classification Parameters for the Emission-line Spectra of Extragalactic Objects, PASP, 93, 5

Donoso, E., et al., 2012, Origin of 12 $\mu$m Emission across Galaxy Populations from *WISE* and SDSS surveys, ApJ, 748, 80

Lee, J. C., Hwang, H. S., Lee, M. G., Kim, M., & Kim, S. C., 2011, Optical Spectral Classification of Southern Ultraluminous Infrared Galaxies, MNRAS, 414, 702

Mullaney, J. R., Alexander, D. M., Goulding, A. D., & Hickox, R. C., 2011, Defining the Intrinsic AGN Infrared Spectral Energy Distribution and Measuring Its Contribution to the Infrared Output of Composite Galaxies, MNRAS, 414, 1082

Veilleux, S., et al., 2009, *SPITZER* Quasar and ULIRG Evolution Study (QUEST). IV. Comparison of 1 Jy Ultraluminous Infrared Galaxies with Palomar-Green Quasars, ApJS, 182, 628